$$+K(z)\Big\}+\frac{1}{2\rho(z)}\frac{\partial}{\partial z}\left\{\frac{E(z)}{1+\sigma(z)}\left[\frac{\partial}{\partial z}\int_0^t\int_0^\vartheta u_{1y}(x,y,z,\tau)\,d\tau\,d\vartheta+\right.\right.$$

$$\left.\left.+\frac{\partial}{\partial y}\int_0^t\int_0^\vartheta u_{1z}(x,y,z,\tau)\,d\tau\,d\vartheta\right]\right\}-K(z)\int_0^t\int_0^\vartheta T(x,y,z,\tau)\,d\tau\,d\vartheta\times$$

$$\times\frac{\beta(z)}{\rho(z)}-\frac{\partial^2}{\partial y\partial z}\int_0^t\int_0^\vartheta u_{1y}(x,y,z,\tau)\,d\tau\,d\vartheta\left\{\frac{E(z)}{6[1+\sigma(z)]}-K(z)\right\}\times$$

$$\times\frac{1}{\rho(z)}-\frac{E(z)}{2\rho(z)[1+\sigma(z)]}\left[\frac{\partial^2}{\partial x^2}\int_0^\infty\int_0^\vartheta u_{1x}(x,y,z,\tau)\,d\tau\,d\vartheta+\right.$$

$$\left.+\frac{\partial^2}{\partial x\partial y}\int_0^\infty\int_0^\vartheta u_{1x}(x,y,z,\tau)\,d\tau\,d\vartheta\right]-K(z)\int_0^\infty\int_0^\vartheta T(x,y,z,\tau)\,d\tau\,d\vartheta\times$$

$$\times\frac{\beta(z)}{\rho(z)}-\frac{1}{\rho(z)}\frac{\partial^2}{\partial y^2}\int_0^\infty\int_0^\vartheta u_{1x}(x,y,z,\tau)\,d\tau\,d\vartheta\left\{\frac{5E(z)}{12[1+\sigma(z)]}+\right.$$

$$\left.+K(z)\right\}-\frac{K(z)}{\rho(z)}\frac{\partial^2}{\partial x\partial y}\int_0^\infty\int_0^\vartheta u_{1y}(x,y,z,\tau)\,d\tau\,d\vartheta-\frac{\partial}{\partial z}\left\{\frac{E(z)}{1+\sigma(z)}\times\right.$$

$$\left.\times\left[\frac{\partial}{\partial z}\int_0^\infty\int_0^\vartheta u_{1y}(x,y,z,\tau)\,d\tau\,d\vartheta+\frac{\partial}{\partial y}\int_0^\infty\int_0^\vartheta u_{1z}(x,y,z,\tau)\,d\tau\,d\vartheta\right]\right\}\times$$

$$\times\frac{1}{2\rho(z)}+\frac{1}{\rho(z)}\frac{\partial^2}{\partial y\partial z}\int_0^\infty\int_0^\vartheta u_{1y}(x,y,z,\tau)\,d\tau\,d\vartheta\left\{\frac{E(z)}{6[1+\sigma(z)]}-\right.$$

$$\left.-K(z)\right\}+u_{0y}$$

$$u_z(x,y,z,t)=\frac{E(z)}{2[1+\sigma(z)]}\left[\frac{\partial^2}{\partial x^2}\int_0^\infty\int_0^\vartheta u_{1z}(x,y,z,\tau)\,d\tau\,d\vartheta+\right.$$

$$+\frac{\partial^2}{\partial y^2}\int_0^\infty\int_0^\vartheta u_{1z}(x,y,z,\tau)\,d\tau\,d\vartheta+\frac{\partial^2}{\partial x\partial z}\int_0^\infty\int_0^\vartheta u_{1x}(x,y,z,\tau)\,d\tau\,d\vartheta+$$

$$\left.+\frac{\partial^2}{\partial y\partial z}\int_0^\infty\int_0^\vartheta u_{1y}(x,y,z,\tau)\,d\tau\,d\vartheta\right]\frac{1}{\rho(z)}+\frac{1}{\rho(z)}\frac{\partial}{\partial z}\left\{K(z)\times\right.$$

$$\times\left[\frac{\partial}{\partial x}\int_0^\infty\int_0^\vartheta u_{1x}(x,y,z,\tau)\,d\tau\,d\vartheta+\frac{\partial}{\partial y}\int_0^\infty\int_0^\vartheta u_{1x}(x,y,z,\tau)\,d\tau\,d\vartheta+\right.$$

$$\left.\left.+\frac{\partial}{\partial z}\int_0^\infty\int_0^\vartheta u_{1x}(x,y,z,\tau)\,d\tau\,d\vartheta\right]\right\}+\frac{1}{6\rho(z)}\frac{\partial}{\partial z}\left\{\frac{E(z)}{1+\sigma(z)}\times\right.$$

$$\times\left[6\frac{\partial}{\partial z}\int_0^\infty\int_0^\vartheta u_{1z}(x,y,z,\tau)\,d\tau\,d\vartheta-\frac{\partial}{\partial x}\int_0^\infty\int_0^\vartheta u_{1x}(x,y,z,\tau)\,d\tau\,d\vartheta-\right.$$

$$\left.\left.-\frac{\partial}{\partial y}\int_0^\infty\int_0^\vartheta u_{1y}(x,y,z,\tau)\,d\tau\,d\vartheta-\frac{\partial}{\partial z}\int_0^\infty\int_0^\vartheta u_{1z}(x,y,z,\tau)\,d\tau\,d\vartheta\right]\right\}-$$

$$-K(z)\frac{\beta(z)}{\rho(z)}\frac{\partial}{\partial z}\int_0^\infty\int_0^\vartheta T(x,y,z,\tau)\,d\tau\,d\vartheta+u_{0z}\,.$$

Framework this paper we determine concentration of dopant, concentrations of radiation defects and components of displacement vector by using the second-order approximation framework method of averaging of function corrections. This approximation is usually enough good approximation to make qualitative analysis and to obtain some quantitative results. All obtained results have been checked by comparison with results of numerical simulations.

3. DISCUSSION

In this section we analyzed dynamics of redistributions of dopant and radiation defects during annealing and under influence of mismatch-induced stress and modification of porosity. Typical distributions of concentrations of dopant in heterostructures are presented on Figures 2 and 3 in direction, which is perpendicular to interface between epitaxial layer substrate. Figure 2 corresponds to diffusion type of doping. Figure 3 corresponds to diffusion type of doping. Increasing of number of curve corresponds to increasing of difference between values of dopant diffusion coefficient in layers of heterostructure under condition, when value of dopant diffusion coefficient in epitaxial layer is larger, than value of dopant diffusion coefficient in substrate. These distributions have been calculated for the case, when value of dopant diffusion coefficient in doped area is larger, than in nearest areas. Curves 1 and 3 on Figure 3 corresponds to annealing time $\Theta=0.0048(L_x^2+L_y^2+L_z^2)/D_0$. Curves 2 and 4 on Figure 3 corresponds to annealing time $\Theta=0.0057(L_x^2+L_y^2+L_z^2)/D_0$. Curves 1 and 2 corresponds to homogenous sample. Curves 3 and 4 corresponds to heterostructure under condition, when value of dopant diffusion coefficient in epitaxial layer is larger, than value of dopant diffusion coefficient in substrate. Annealing time of dopant, which corresponds to Figure 2, is equal to $\Theta=0.005(L_x^2+L_y^2+L_z^2)/D_0$. The figures show, that inhomogeneity of heterostructure gives us possibility to increase compactness of concentrations of dopants and at the same time to increase homogeneity of dopant distribution in doped part of epitaxial layer. However, this manufacturing approach of bioplar transistor cannot effectively anneal the dopants and/or radiation defects. The annealing process should be optimized for the following reasons. If annealing time is small, the dopant did not achieve any interfaces between materials of heterostructure. In this situation one cannot find any modifications of distribution of concentration of dopant. If annealing time is large, distribution of concentration of dopant is too homogenous. We optimize annealing time framework recently introduces approach [29-37]. Framework this criterion we approximate real distribution of concentration of dopant by step-wise function (see Figures 4 and 5). These figures show spatial distributions of dopant in heterostructure after infusion (for Figure 4) or implantation of dopant (for Figure 5). Curve 1 is idealized distribution of dopant. Curves 2-4 are real distributions of dopant for different values of annealing time. Increasing of number of curve corresponds to increasing of annealing time. Farther we determine optimal values of annealing time by minimization of the following mean-squared error.

$$U=\frac{1}{L_xL_yL_z}\int_0^{L_x}\int_0^{L_y}\int_0^{L_z}\left[C(x,y,z,\Theta)-\psi(x,y,z)\right]\,d\,z\,d\,y\,d\,x \quad (22)$$

where, $\psi(x,y,z)$ is the approximation function. Dependences of optimal values of annealing time on parameters are presented on Figures 6 and 7 for diffusion and ion types of doping, respectively. Curve 1 is the dependence of dimensionless optimal annealing time on the relation a/L and $\xi=\gamma=0$ for equal to each other values of dopant diffusion coefficient in all parts of heterostructure. Curve 2 is the dependence of dimensionless optimal annealing time on value of parameter ε for $a/L=1/2$ and $\xi=\gamma=0$. Curve 3 is the dependence of dimensionless optimal annealing time on value of parameter ξ for $a/L=1/2$ and $\varepsilon=\gamma=0$. Curve 4 is the dependence of dimensionless optimal annealing time on value of parameter γ for $a/L=1/2$ and $\varepsilon=\xi=0$. It should be noted, that

it is necessary to anneal radiation defects after ion implantation. One could find spreading of concentration of distribution of dopant during this annealing. In the ideal case distribution of dopant achieves appropriate interfaces between materials of heterostructure during annealing of radiation defects. If dopant did not achieve any interfaces during annealing of radiation defects, it is practicably to additionally anneal the dopant. In this situation optimal value of additional annealing time of implanted dopant is smaller, than annealing time of infused dopant.

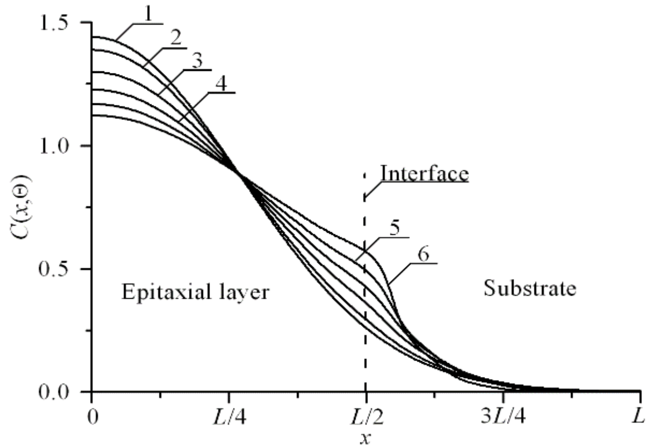

Figure 2. Distributions of concentration of infused dopant

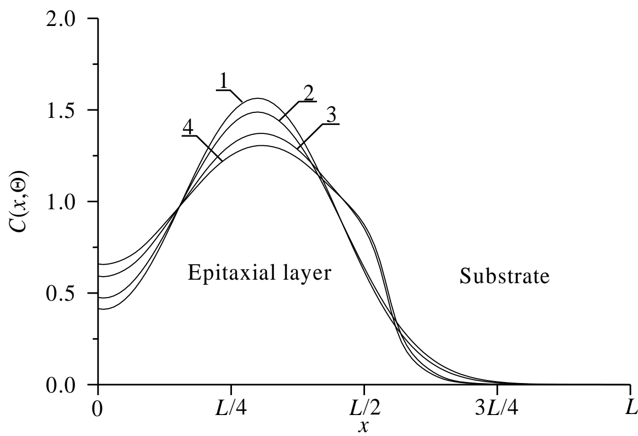

Figure 3. Distributions of concentration of implanted dopant

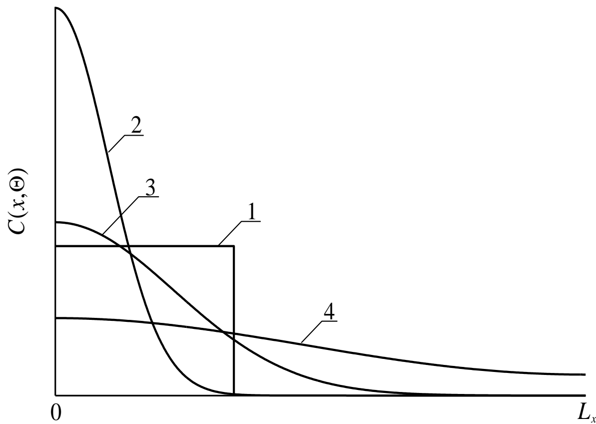

Figure 4. Typical spatial distributions of dopant in heterostructure after dopant infusion

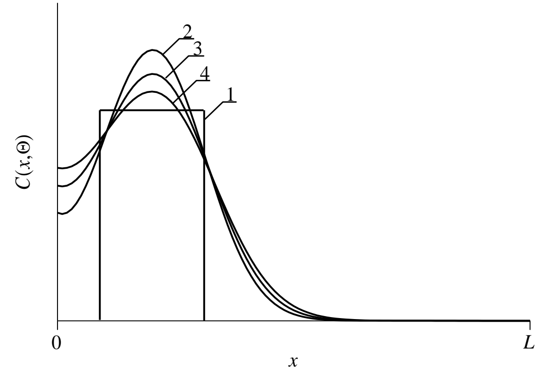

Figure 5. Typical spatial distributions of dopant in heterostructure after ion implantation

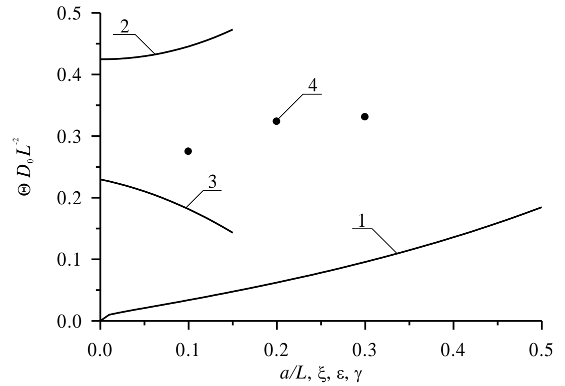

Figure 6. Dependences of dimensionless optimal annealing time for doping by diffusion

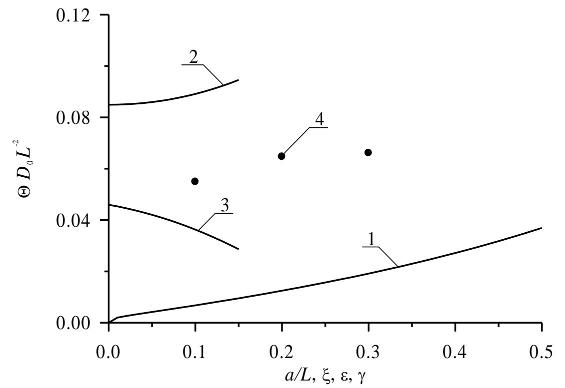

Figure 7. Dependences of dimensionless optimal annealing time for doping by ion implantation

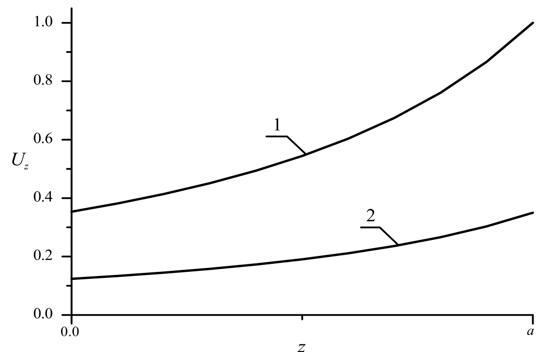

Figure 8. Normalized dependences of component u_z of displacement vector on coordinate z for nonporous (curve 1) and porous (curve 2) epitaxial layers

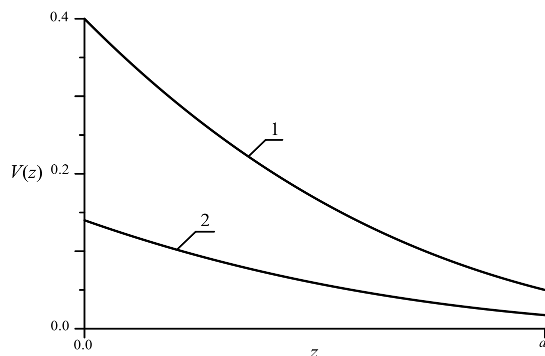

Figure 9. Normalized dependences of vacancy concentrations on coordinate z in unstressed (curve 1) and stressed (curve 2) epitaxial layers

Farther we analyzed influence of relaxation of mechanical stress on distribution of dopant in doped areas of heterostructure. Under following condition $\varepsilon_0< 0$ one can find compression of distribution of concentration of dopant near interface between materials of heterostructure. Contrary (at $\varepsilon_0>0$) one can find spreading of distribution of concentration of dopant in this area. This changing of distribution of concentration of dopant could be at least partially compensated by using laser annealing [37]. This type of annealing gives us possibility to accelerate diffusion of dopant and other processes in annealed area due to inhomogenous distribution of temperature and Arrhenius law. Accounting relaxation of mismatch-induced stress in heterostructure could leads to changing of optimal values of annealing time. At the same time modification of porosity gives us possibility to decrease value of mechanical stress. On the one hand mismatch-induced stress could be used to increase density of elements of integrated circuits. On the other hand, it could leads to generation dislocations of the discrepancy. Figures 8 and 9 show distributions of concentration of vacancies in porous materials and component of displacement vector, which is perpendicular to interface between layers of heterostructure.

4. CONCLUSION

In this paper we model redistribution of infused and implanted dopants with account relaxation mismatch-induced stress during manufacturing field-effect heterotransistors framework a two-level current-mode logic gates in a multiplexer. We obtain, that using difference between materials of heterostructure and optimization of annealing of dopant and/or radiation defects gives a possibility to decrease dimensions of transistors and to increase their density. We obtain, that using ion implantation gives a possibility to decrease mismatch-induced stress. At the same time, it is necessary to choose materials with higher charge carrier motility and minimal mismatch-induced stress. Minimization of mismatch-induced stress gives a possibility to use diffusion type of doping without radiation damage of materials of heterostructure. Increasing of charge carrier motility gives a possibility to accelerate of transport of charge carriers. We also introduce an analytical approach to model diffusion and ion types of doping with account concurrent changing of parameters in space and time. At the same time the approach gives us possibility to take into account nonlinearity of considered processes.

REFERENCES

[1] Lachin, V.I., Savelov, N.S. (2001). Electronics. Phoenix. Rostov-on-Don.

[2] Polishscuk, A. (2004). Anadigm Programmable analog integrated circuits: The entire spectrum of analog electronics on a single chip. First meeting. Modern Electronics, 12: 8-11.

[3] Volovich, G. (2006). Modern chips UM3Ch class D manufactured by firm MPS. Modern Electronics, 2: 10-17.

[4] Kerentsev, A., Lanin, V. (2008). Constructive-technological features of MOSFET-transistors. Power Electronics, 1: 34-38.

[5] Ageev, A.O., Belyaev, A.E., Boltovets, N.S., Ivanov, V.N., Konakova, R.V., Kudrik, Ya.Ya., Litvin, P.M., Milenin, V.V., Sachenko, A.V. (2009). Au-TiB_x-n-6H-SiC Schottky barrier diodes: the features of current flow in rectifying and nonrectifying contacts. Semiconductors, 43(7): 865-871. https://doi.org/10.1134/S1063782609070070

[6] Tsai, J.H., Chiu, S.Y., Lour, W.S. Guo, D.F. (2009). High-performance InGaP/GaAs PNP δ-doped heterojunction bipolar transistor. Semiconductors, 43(7): 939-942. https://doi.org/10.1134/S1063782609070227

[7] Alexandrov, O.V., Zakhar'in, A.O., Sobolev, N.A., Shek, E.I., Makoviychuk, M.M., Parshin, E.O. (1998). Formation of donor centers upon annealing of dysprosium-and holmium-implanted silicon. Semiconductors, 32(9): 921-923. https://doi.org/10.1134/1.1187515

[8] Ermolovich, I.B., Milenin, V.V., Red'ko, R.A., Red'ko, S.M. (2009). Specific features of recombination processes in CdTe films produced in different temperature conditions of growth and subsequent annealing. Semiconductors, 43(8): 980-984. https://doi.org/10.1134/S10 6378260908003X

[9] Sinsermsuksakul, P., Hartman, K., Kim, S.B., Heo, J., Sun, L., Park, H.H., Chakraborty, R., Buonassisi, T., Gordon, R.G. (2013). Enhancing the efficiency of SnS solar cells via band-offset engineering with a zinc oxysulfide buffer layer. Applied Physics Letters, 102(5): 053901-053905. https://doi.org/10.1063/1.4789855

[10] Reynolds, J.G., Reynolds, C.L., Mohanta, Jr.A., Muth, J.F., Rowe, J.E., Everitt, H.O., Aspnes, D.E. (2013). Shallow acceptor complexes in *p*-type ZnO. Applied Physics Letters, 102(15): 152114-152118. https://doi.org/10.1063/1.4802753

[11] Volokobinskaya, N.I., Komarov, I.N., Matyukhina, T.V., Reshetnikov, V.I., Rush, A.A., Falina, I.V., Yastrebov, A.S. (2001). A study of technological processes in the production of high-power high-voltage bipolar transistors incorporating an array of inclusions in the collector region. Semiconductors, 35(8): 974-978. https://doi.org/10.1134/1.1393038

[12] Pankratov, E.L., Bulaeva, E.A. (2013). Doping of materials during manufacture *p-n*-junctions and bipolar transistors. Analytical approaches to model technological approaches and ways of optimization of distributions of dopants. Reviews in Theoretical Science, 1(1): 58-82. https://doi.org/10.1166/rits.2013.1004

[13] Kukushkin, S.A., Osipov, A.V., Romanychev, A.I. (2016). Epitaxial growth of zinc oxide by the method of atomic layer deposition on SiC/Si substrates. Physics of

the Solid State, 58(7): 1448-1452. https://doi.org/10.1134/S1063783416070246

[14] Trukhanov, E.M., Kolesnikov, A.V., Loshkarev, I.D. (2015). Long-range stresses generated by misfit dislocations in epitaxial films. Russian Microelectronics, 44(8): 552-558. https://doi.org/10.1134/S1063739715080 119

[15] Pankratov, E.L., Bulaeva, E.A. (2015). On optimization of regimes of epitaxy from gas phase. Some analytical approaches to model physical processes in reactors for epitaxy from gas phase during growth films. Reviews in Theoretical Science, 3(4): 365-398. https://doi.org/10.1166/rits.2015.1041

[16] Ong, K.K., Pey, K.L., Lee, P.S., Wee, A.T.S., Wang, X.C., Chong, Y.F. (2006). Dopant distribution in the recrystallization transient at the maximum melt depth induced by laser annealing. Applied Physics Letters, 89 (17): 172111-172114. https://doi.org/10.1063/1.2364834

[17] Wang, H.T., Tan, L.S., Chor, E.F. (2005). Pulsed laser annealing of Be-implanted GaN. Journal of Applied Physics, 98(9): 094901-094905. https://doi.org/10.1063/1.2120893

[18] Bykov, Y.V., Yeremeev, A.G., Zharova, N.A., Plotnikov, I.V., Rybakov, K.I., Drozdov, M.N., Drozdov, Y.N., Skupov, V.D. (2003). Diffusion processes in semiconductor structures during microwave annealing. RadioPhysics and Quantum Electronics, 43(9): 749-755. https://doi.org/10.1023/B:RAQE.0000025008.97954.1c

[19] Jang, I., Kim, J., Kim, S. (2015). Accurate delay models of CMOS CML circuits for design optimization. Analog Integrated Circuits and Signal Processing, 82(1): 297-307. https://doi. org/10.1007/s10470-014-0460-4

[20] Zhang, Y.W., Bower, A.F. (1999). Numerical simulations of island formation in a coherent strained epitaxial thin film system. Journal of the Mechanics and Physics of Solids, 47(11): 2273-2297. https://doi.org/10.1016/S0022-5096(99)00026-5

[21] Landau, L.D., Lefshits, E.M., Kosevich, A.M., Pitaevskii, L.P. (2001). Theoretical Physics. 7 (Theory of elasticity). Physmatlit, Moscow.

[22] Kitayama, M., Narushima, T., Carter, W.C., Cannon, R.M., Glaeser, A.M. (2000). The Wulff shape of alumina: I, modeling the kinetics of morphological evolution. Journal of the American Ceramic Society, 83(10): 2561-2531. https://doi.org/10.1111/j.1151-2916.2000.tb01591.x

[23] Cheremskoy, P.G., Slesov, V.V., Betekhtin, V.I. (1990). Pore in solid bodies. Energoatomizdat, Moscow.

[24] Gotra, Z.Y. (1991). Technology of microelectronic devices. Radio and Communication, Moscow.

[25] Fahey, P.M., Griffin, P.B., Plummer, J.D. (1989). Point defects and dopant diffusion in silicon. Reviews of Modern Physics, 61(2): 289-388. https://doi.org/10.1103/RevModPhys.61. 289

[26] Vinetskiy, V.L., Kholodar', G.A. (1979). Radiative physics of semiconductors. Naukova Dumka, Kiev.

[27] Mynbaeva, M.G., Mokhov, E.N., Lavrent'ev, A.A., Mynbaev, K.D. (2008). High-temperature diffusion doping of porous silicon carbide. Technical Physics Letters, 34(9): 13. https://doi.org/10.1134/S106378500809 0034

[28] Sokolov, Y.D. (1955). About the definition of dynamic forces in the mine lifting. Applied Mechanics, 1(1): 23-35.

[29] Pankratov, E.L. (2007). Dopant diffusion dynamics and optimal diffusion time as influenced by diffusion-coefficient nonuniformity. Russian Microelectronics, 36(1): 33-39. https://doi.org/10.1134/S1063739707010040

[30] Pankratov, E.L. (2008). Redistribution of a dopant during annealing of radiation defects in a multilayer structure by laser scans for production of an implanted-junction rectifier. International Journal of Nanoscience, 7(4-5): 187-197. https://doi.org/10.1142/S0219581X08 005328

[31] Pankratov, E.L., Bulaeva, E.A. (2013). Doping of materials during manufacture *p-n*-junctions and bipolar transistors. Analytical approaches to model technological approaches and ways of optimization of distributions of dopants. Reviews in Theoretical Science, 1(1): 58-82. https://doi.org/10.1166/rits.2013.1004

[32] Pankratov, E.L., Bulaeva, E.A. (2012). Decreasing of quantity of radiation defects in an implanted-junction rectifiers by using overlayers. Int. J. Micro-Nano Scale Transp., 3(3): 119-130.

[33] Pankratov, E.L., Bulaeva, E.A. (2015). Optimization of manufacturing of emitter-coupled logic to decrease surface of chip. International Journal of Modern Physics B, 29(5): 1-12. https://doi.org/10.1142/S021797921550023X

[34] Pankratov, E.L. (2017). On approach to optimize manufacturing of bipolar heterotransistors framework circuit of an operational. Amplifier to increase their integration rate. influence mismatch-induced stress. J. Comp. Theor. Nanoscience, 14(10): 4885-4899. https://doi.org/10.1166/jctn.2017.6899

[35] Pankratov, E.L., Bulaeva, E.A. (2015). An approach to increase the integration rate of planar drift heterobipolar transistors. Materials Science in Semiconductor Processing, 34: 260-268. https://doi.org/10.1016/j.mssp.2015.02. 054

[36] Pankratov, E.L., Bulaeva, E.A. (2014). An approach to manufacture of bipolar transistors in thin film structures. On the method of optimization. International Journal of Micro-Nano Scale Transport, 4(1): 17-31.

[37] Pankratov, E.L., Bulaeva, E.A. (2016). An analytical approach for analysis and optimization of formation of field-effect heterotransistors. Multidiscipline Modeling in Materials and Structures, 12(4): 578-604. https://doi.org/10.1108/MMMS-09-2015-0057